Kinetic Studies of the Interaction of Bromphenol Blue with Bovine Serum Albumin by Pressure-jump Method

Kiyofumi MURAKAMI, Takayuki SANO, and Tatsuya YASUNAGA*

Department of Chemistry, Faculty of Science, Hiroshima University, Higashisenda-machi, Naka-ku, Hiroshima 730

(Received August 5, 1980)

The interaction of Bromphenol Blue (BPB) with bovine serum albumin (BSA) was studied statically, by spectrophotometry, and kinetically, by the pressure-jump method. The absorbance changes of BPB were monitored at 20 °C, pH 7.00 in 0.2 M† phosphate buffer. The static measurements showed that there were two binding classes. The number of binding sites and the binding constants for each class are $n_1=1$, $K_1=1.4\times10^7$ M^{-1} and $n_2=3$, $K_2=9.5\times10^4$ M^{-1}. Kinetically, the binding of BPB to the primary binding site of BSA proceeds *via* at least 4 steps. Two models are offered for the possible binding mechanism. In these models, a fast, probably diffusion controlled, second order step is followed by three first order steps. A correlation between the number of binding steps and the magnitude of the binding constant is discussed. The positive activation entropies associated with the backward reactions of the second and third steps show that these reactions proceed through disordered activation states. From the comparison of the present results to those for other ligands, it was found that the ligand is intimately involved in which activated configuration is adopted.

Albumin reversibly binds many kinds of small molecules such as fatty acids, bilirubin, amino acids, drugs and hormones, and plays important roles as carrier and buffer for these molecules. The binding of albumin with small molecules, therefore, is one important factor which determines the distribution, metabolism and excretion of small molecules in the body. It has been extensively studied by static methods.

On the other hand, until the past few years, the kinetics of the interactions of albumin with small molecules had not been extensively studied since the investigation of Froese *et al.*,[1] probably because the binding of small molecules with albumin was thought to be too fast to be a rate-limiting process in physiological phenomena.[2,3] However, recently, many kinetic studies have been performed in the attempt to elucidate the detailed binding mechanism of physiologically important substances such as bilirubin[4-8] and fatty acid.[9]

The interactions of organic dyes with albumin have often been studied as the model systems of protein-small molecule interaction. Besides the role of a model system, the binding of Bromphenol Blue with albumin has physiologically and clinically important applications such as the quantitative analyses of proteins[10] and the determination of the concentration of available bilirubin binding sites in serum[11,12] using the spectrum shift of Bromphenol Blue on binding to albumin. The investigation of the detailed binding mechanism may offer a better basis for such procedures.

In the present study, the binding mechanism of Bromphenol Blue to bovine serum albumin was investigated through both static and kinetic experiments. The kinetic study was concerned with binding to the highest affinity site, which is the most important site for physiological effects.

Experimental

Materials. Bovine serum albumin fraction V(BSA) was obtained from Armour Laboratories and was used without further purifications. The dimer content was about 5%, as determined by gel chromatography with Sephadex G-150. The fatty acid content was determined to be 0.33 mole per mole of protein by the method of Dole.[13] The BSA solutions were prepared by weight, assuming a molecular weight of 69000. Bromphenol Blue (BPB) was of special reagent grade from Wako Pure Chemical Industries, Ltd. and recrystallized from a mixture of acetone and acetic acid. All other chemicals used were reagent grade and used without further purification. All the sample solutions were prepared in 0.2 M phosphate buffer of pH 7.00.

Apparatus. The absorption spectra were measured with a Union Giken SM401 Spectrophotometer. The kinetic measurements were performed with an optical detection pressure-jump apparatus constructed in our laboratory. The pressure of the sample solution was suddenly decreased from 150 atm to 1 atm by rupture of brass film within a time of 100 μs. The light source used was a halogen lamp (250 W) and the path length of the cell was 10 mm. The details of the pressure-jump apparatus can be found elsewhere.[14] All measurements were performed at 20±0.2 °C with the exception of the experiments on the temperature dependence of the relaxation times.

Results

Spectrophotometric Studies. The absorption spectra of the BSA–BPB complex under the various polymer-to-dye ratios (P/D) are shown in Fig. 1. The peak of the spectrum of the free dye around 590 nm decreases with increasing P/D, and that of the complex at 610 nm increases. The increase of the absorbance in the whole range of wavelength with the change of P/D from 4 to 20 shows that the contribution of the absorbance of the protein can not be ignored. The binding parameters were determined from the absorbance change at 590 nm by applying the correction for the contribution of the protein. The extinction coefficients of the free and bound dyes were determined to be $\varepsilon_f=7.9\times10^4$ M^{-1} cm^{-1} and $\varepsilon_b=4.5\times10^4$ M^{-1} cm^{-1} respectively. The latter value was determined from the absorbance at the higher limit of P/D. The concentration of the free dye C and the average number of bound dye molecules per molecule of BSA $\bar{\nu}$ were determined from the equations:

† In this paper 1 M=1 mol dm^{-3}.

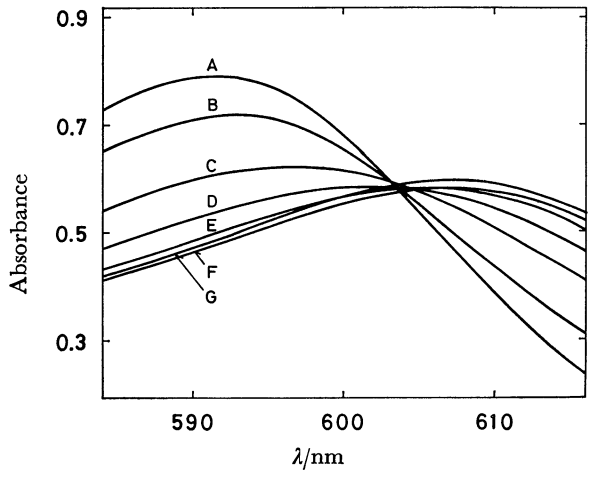

Fig. 1. P/D dependence of absorption spectra of BPB–BSA complex at 20 °C, pH 7.00 and $C_0=1\times10^{-5}$ M. A: Dye only, B: P/D=0.1, C: P/D=0.3, D: P/D=0.5, E: P/D=1, F: P/D=4, G: P/D=20.

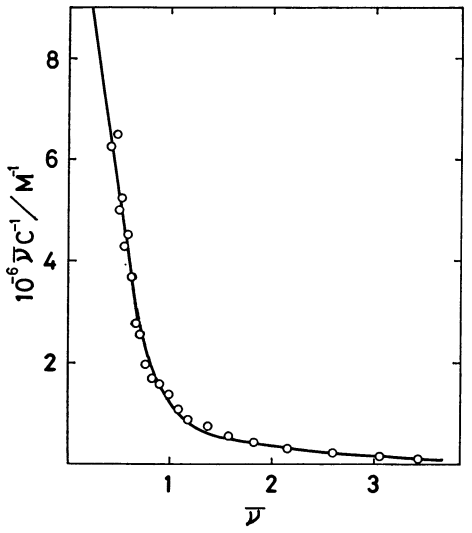

Fig. 2. Scatchard plot of the binding of BPB to BSA.

$$C=\frac{\varepsilon_{app}-\varepsilon_b}{\varepsilon_f-\varepsilon_b}C_0, \tag{1}$$

$$\bar{\nu}=\frac{C_0-C}{P_0}, \tag{2}$$

with

$$\varepsilon_{app}=\frac{A}{C_0 l},$$

where C_0 and P_0 are the total concentrations of the dye and the polymer, respectively, A is the absorbance at 590 nm, and l is the path length of the cell. The Scatchard plot[15] for the present system is shown in Fig. 2. The analysis of this plot yields the following binding parameters:

$$n_1=0.8, \qquad K_1=1.4\times10^7\ M^{-1},$$

$$n_2=3.4, \qquad K_2=9.5\times10^4\ M^{-1},$$

where n_1 and n_2 are the number, of binding sites for the primary and secondary binding sites, respectively. The solid line in Fig. 2 represents the theoretical curve calculated using these values. Good agreement can be seen between the observed and calculated curves. For the calculation of equilibrium concentrations, we used $n_1=1$, $n_2=3$, since these are the closest integers to 0.8 and 3.4.

In the present study, the number of binding sites and the equilibrium constants were determined using the absorbance at the wavelength 590 nm with the same extinction coefficient for all kinds of complexes. At this wavelength, the absorbance decreases to the saturation value with increasing concentration of BSA, and reaches saturation at P/D$\simeq$5. On the other hand, at the wavelength 610 nm, where the absorbance increases with the concentration of BSA, a gradual increase of the absorbance was observed above P/D$\simeq$5. This effect is probably due to dimer formation, which makes the environment around BPB more hydrophobic. This can also be presumed from the fact that the effect becomes more pronounced in more concentrated solutions.

The binding isotherm of BPB with BSA has also been investigated by other researchers. Bjerrum[16] has obtained $n_1=3$, $K_1=5\times10^5\ M^{-1}$, and $n_2=4$, $K_2=2.5\times10^4\ M^{-1}$ at 4.5 °C, pH 7.00 in 0.1 M phosphate buffer by the gel chromatography method. His studies were confined to values of $\bar{\nu}$ above 1; the primary binding sites in his study may thus correspond to the secondary binding sites in the present study. Peeters *et al.*[7] have reported $n_1=1$, $K_1=7.8\times10^5\ M^{-1}$, $n_2=3$, $K_2=7.6\times10^3\ M^{-1}$, $n_3=12$, $K_3=3.1\times10^2\ M^{-1}$ with the defatted BSA at 25 °C, pH 6.62 in 0.1 M phosphate buffer using the microcalorimetry method. The number of binding sites for both of the stronger two binding classes agrees with those of the present study, but the binding constants are about one order of magnitude smaller. The differences in the binding constants may be due to differences in the fatty acid content[7] and/or pH.[18]

Kinetic Studies. Four separate relaxation processes could be observed. The relaxation amplitudes were very small, and 4 to 20 repetitions were averaged to measure the relaxation times. Typical relaxation curves observed at 540 nm are shown in Fig. 3. These relaxations were observed from 400 nm to 560 nm. The relaxation time of the fastest process, which appears as the sudden decrease at $t=0$ in Fig. 3(a), was shorter than the time constant of the apparatus and could not be measured even at a temperature of 5 °C. To obtain the relaxation time of the fastest process, temperature-jump measurements with a temperature increase of about 2 degrees were tried for the same samples, but no relaxation was observed. The static absorption spectra were also insensitive to temperature. All relaxations were observed at 610 nm with opposite direction to and same relaxation times as those observed in the shorter wavelength region. In addition to these four relaxation processes, a relaxational phenomenon with a longer time constant, around 1 min, was observed. This phenomenon has a very small relaxation amplitude, and could be seen only for relatively concentrated samples. Therefore, this phenomenon was not discussed in the present study. These four relaxation processes were numbered 1, 2, 3, 4 in order of the relaxation times,

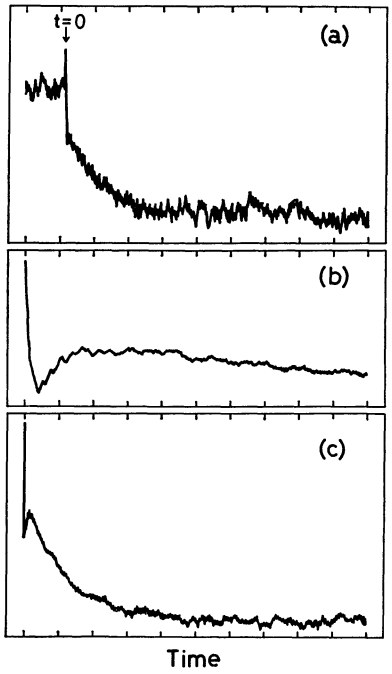

Fig. 3. Typical relaxation spectra of the BPB-BSA system at 20 °C, pH 7.00, λ=540 nm, $C_0=1\times10^{-5}$ M, and $P_0=2\times10^{-5}$ M.
(a) 2ms/div., (b) 40ms/div., (c) 400ms/div.

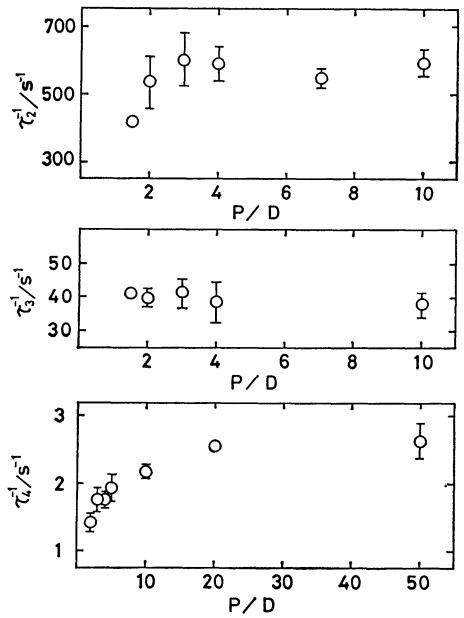

Fig. 4. P/D dependences of the reciprocal relaxation times for slower three processes.

from fast to slow.

Interpretation of the Kinetic Data. The P/D dependences of the relaxation times of the slower three processes, 2, 3, 4 in the region of P/D>1, where the binding of the dye to the highest affinity site of protein occurs, are shown in Fig. 4. All these processes show saturation behavior with P/D. This fact shows that these processes are essentially first order processes. Considering the existences of the very fast process and the three first order processes, the following six models, which are the simplest available under the assumption that the extinction coefficients of the complexes are equal, were examined.

First, the series model which is represented by Eq. 3 was examined.

Model 1

$$\mathrm{D} + \mathrm{P} \underset{k_{-1}}{\overset{k_1}{\underset{\longleftarrow}{\overset{\longrightarrow}{K_1'}}}} \mathrm{C}_1 \underset{k_{-2}}{\overset{k_2}{\underset{\longleftarrow}{\overset{\longrightarrow}{K_2'}}}} \mathrm{C}_2 \underset{k_{-3}}{\overset{k_3}{\underset{\longleftarrow}{\overset{\longrightarrow}{K_3'}}}} \mathrm{C}_3 \underset{k_{-4}}{\overset{k_4}{\underset{\longleftarrow}{\overset{\longrightarrow}{K_4'}}}} \mathrm{C}_4, \qquad (3)$$

very fast fast slow very slow

where D, P, and C_i denote free dye, free polymer and complexes of the dye and the polymer, respectively, K_i' is the equilibrium constant, and k_i and k_{-i} are the forward and backward rate constants, respectively. The relaxation times and the overall equilibrium constant for this model are expressed by

$$\tau_1^{-1} = k_1(C+P) + k_{-1} \qquad (4)$$

$$\tau_2^{-1} = k_2\frac{K_1'(C+P)}{1+K_1'(C+P)} + k_{-2} \qquad (5)$$

$$\tau_3^{-1} = k_3\frac{K_1'K_2'(C+P)}{1+K_1'(1+K_2')(C+P)} + k_{-3} \qquad (6)$$

$$\tau_4^{-1} = k_4\frac{K_1'K_2'K_3'(C+P)}{1+K_1'\{1+K_2'(1+K_3')\}(C+P)} + k_{-4} \qquad (7)$$

$$K_\Sigma = K_1'\{1+K_2'(1+K_3'(1+K_4'))\}. \qquad (8)$$

The relaxation time τ_1 of the fast bimolecular step could not be obtained in the present experiment, so that it is difficult to determine all the constants of each reaction step from the fast to slow step successively. Moreover, the experimental errors of the relaxation times are relatively large. Thus, the validity of the reaction mechanism was examined from the standpoint of determining whether proper constants satisfying the concentration dependences of the relaxation times could be chosen. First, from the data of τ_2 and τ_4, the allowable ranges of the combinations of the parameters were estimated as follows:

k_2K_1'	1×10^7—2.6×10^8 M^{-1} s^{-1}
K_1'	3.3×10^4—4.4×10^5 M^{-1}
k_{-2}	0—400 s^{-1}
$k_4K_1'K_2'K_3'$	3.1×10^4—2×10^5 M^{-1} s^{-1}
$K_1'\{1+K_2'(1+K_3')\}$	1.9×10^4—1×10^5 M^{-1}
k_{-4}	0—1.4 s^{-1}.

Next, we get $3.3\times10^4\ M^{-1}\leqslant K_1'\leqslant7\times10^4\ M^{-1}$ from the condition $K_3'\geqslant0$. Using $5\times10^4\ M^{-1}$ as the value of K_1' from the reduced range, the range of K_2' was estimated to be $0.5\leqslant K_2'\leqslant1$. In this range, the value of K_2' which satisfies the concentration dependence of τ_2 is 0.5 (k_2=200 s^{-1}, k_{-2}=400 s^{-1}). From the τ_3 data, we get $K_3'\leqslant0.05$($k_3\leqslant2$ s^{-1}, k_{-3}=40 s^{-1}) using the above values for K_1' and K_2'. Furthermore, we get $K_4'\geqslant1.1\times10^4$ ($k_4\geqslant160$ s^{-1}, 2.3×10^{-3} $s^{-1}\leqslant k_{-4}\leqslant1.5\times10^{-2}$ s^{-1}) using the overall equilibrium constant $K_\Sigma=1.4\times10^7\ M^{-1}$ which was determined as the equilibrium constant for the primary binding site by the spectrophotometric measurements. The results are summarized in Table 1. The comparison of the plots of the reciprocal relaxation times *versus* $K_1'(C+P)$/

Table 1. Equilibrium and rate constants and activation parameters for Models 1 and 5

Step	K_i'	k_i	$\frac{k_{-i}}{s^{-1}}$	$\frac{\Delta H_{-i}^*}{kcal\ mol^{-1}}$	$\frac{\Delta S_{-i}^*}{cal\ mol^{-1}\ K^{-1}}$
		Model 1			
1	$5\times10^4\ M^{-1}$	$>4\times10^8\ M^{-1}\ s^{-1}$	$>8\times10^3$		
2	0.5	$200\ s^{-1}$	400	19	17
3	$\ll0.05$	$\leqslant2\ s^{-1}$	40	36	71
4	$\gg1.1\times10^4$	$\geqslant160\ s^{-1}$	2.3×10^{-3}—1.5×10^{-2}		
		Model 5			
4	280	$1.5\ s^{-1}$	5.4×10^{-3}		

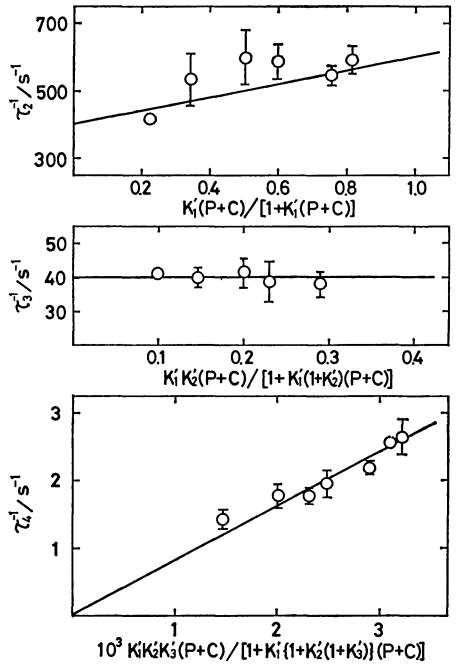

Fig. 5. Plots of the reciprocal relaxation times with Model 1.

$\{1+K_1'(C+P)\}$ for τ_2, $K_1'K_2'(C+P)/\{1+K_1'(1+K_2')(C+P)\}$ for τ_3, and $K_1'K_2'K_3'(C+P)/[1+K_1'\{1+K_2'(1+K_3')\}(C+P)]$ for τ_4 between observed and calculated relaxation times are shown in Fig. 5, in which the solid lines were calculated using the following values: $K_1'=5\times10^4\ M^{-1}$, $K_2'=0.5$ ($k_2=200\ s^{-1}$, $k_{-2}=400\ s^{-1}$), $K_3'=0.01$ ($k_3=0.4\ s^{-1}$, $k_{-3}=40\ s^{-1}$) and $K_4'=5.6\times10^4$ ($k_4=800\ s^{-1}$, $k_{-4}=1.5\times10^{-2}\ s^{-1}$). As can be seen, the theoretical and experimental plots agree relatively well. Therefore, Model 1 seems to be possible as the reaction mechanism of the present system.

Next, the branch model was examined.

Model 2

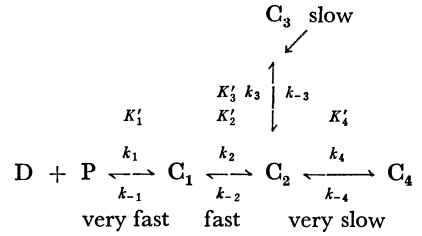

(9)

The relaxation times and the overall equilibrium constant for this model become

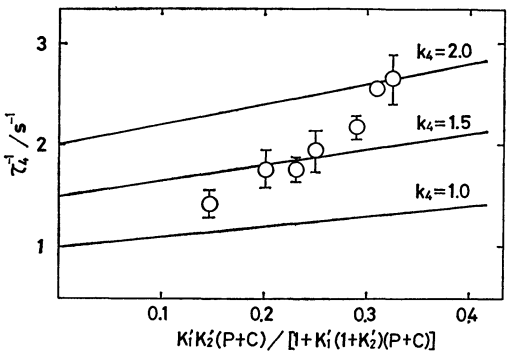

Fig. 6. Plot of τ_4^{-1} with Model 2.

$$\tau_1^{-1} = k_1(C+P) + k_{-1} \tag{10}$$

$$\tau_2^{-1} = k_2\frac{K_1'(C+P)}{1+K_1'(C+P)} + k_{-2} \tag{11}$$

$$\tau_3^{-1} = k_3\frac{K_1'K_2'(C+P)}{1+K_1'(1+K_2')(C+P)} + k_{-3} \tag{12}$$

$$\tau_4^{-1} = k_4\left\{\frac{K_1'K_2'(C+P)}{1+K_1'(1+K_2')(C+P)}+\frac{1}{1+K_3'}\right\} + k_{-4} \tag{13}$$

$$K_\Sigma = K_1'\{1+K_2'(1+K_3'+K_4')\}. \tag{14}$$

The parameters of the Model 2 were determined as follows from an analysis similar to that used in the case of Model 1.

K_1' $5\times10^4\ M^{-1}$

K_2' 0.5 ($k_2=200\ s^{-1}$, $k_{-2}=400\ s^{-1}$)

K_3' $\ll0.05$ ($k_3\ll2\ s^{-1}$, $k_{-3}=40\ s^{-1}$)

K_4' 560 ($1.2\ s^{-1}\ll k_4\ll8\ s^{-1}$, $1.8\times10^{-3}\ s^{-1}\ll k_{-4}\ll1.4\times10^{-2}\ s^{-1}$).

The expressions of the relaxation times of the faster three processes are the same as those of Model 1, so that the same results were obtained for these processes. Since the allowable values of K_3' and k_{-4} do not contribute to the value of τ_4^{-1}, the comparison of the plot of τ_4^{-1} against $K_1'K_2'(C+P)/\{1+K_1'(1+K_2')(C+P)\}$ between observed and calculated relaxation times for some allowable values of k_4 was made as shown in Fig. 6. Model 2 does not explain the concentration dependence of τ_4, so it may be excluded from possible mechanisms of the present system.

In the same way, the following models were also examined.

Model 3

$$\begin{array}{ccccccc} & & & & C_2 & & \\ & & & & \uparrow\downarrow \text{fast} & & \\ D + P & \longleftrightarrow & C_1 & \longleftrightarrow & C_3 & \longleftrightarrow & C_4 \\ & & \text{very fast} & & \text{slow} & & \text{very slow} \end{array}$$

Model 4

$$\begin{array}{ccccccc} & & & & C_3 & & \\ & & & & \uparrow\downarrow \text{slow} & & \\ D + P & \longleftrightarrow & C_1 & \longleftrightarrow & C_2 & \longleftrightarrow & C_4 \\ & & \text{very fast} & & \text{fast} & & \text{very slow} \end{array}$$

Model 5

$$\begin{array}{ccccccc} & & & & C_4 & & \\ & & & & \uparrow\downarrow \text{very slow} & & \\ D + P & \longleftrightarrow & C_1 & \longleftrightarrow & C_2 & \longleftrightarrow & C_3 \\ & & \text{very fast} & & \text{fast} & & \text{slow} \end{array}$$

Model 6

$$\begin{array}{ccccccc} & & & & C_3 & & \\ & & & & \uparrow\downarrow \text{slow} & & \\ D + P & \longleftrightarrow & C_1 & \longleftrightarrow & C_2 & & \\ & & \text{very fast} & \uparrow\downarrow & \text{fast} & & \\ & & & \nwarrow & & & \\ & & & C_4 & \text{very slow} & & \end{array}$$

The concentration dependences of the relaxation times of the second and the third processes can be explained by all of those models, as in the cases of Model 1 and Model 2. Thus, the validity of these models was checked by calculating the concentration dependency of τ_4. The results are shown in Fig. 7 to 10 for the models from 3 to 6, respectively. In these models, only Model 5 can explain the concentration dependence of τ_4. The values of the parameters which were determined with Model 5 are summarized in Table 1, omitting the values for the faster three steps which are same as those of Model 1. From the above analyses, both Model 1 and Model 5 are left as the possible mechanisms from the point of view of the concentration dependences of the relaxation times.

The activation parameters were determined from the temperature dependences of the relaxation times. From the results of the analysis of the reaction mechanism, it was found that the relaxation times whose temperature dependences can be attributed to particular rate constants are τ_2 and τ_3, and the corresponding rate constants are k_{-2} and k_{-3}, respectively. The Eyring plots of those rate constants are shown in Fig. 11. From the slope and the intercept, the activation enthalpy $\Delta H^{\ddagger}_{-3}$ and the entropy $\Delta S^{\ddagger}_{-3}$ of the backward reaction of the second step were determined to be 19 kcal/mol and 17 cal/mol K, respectively, and those of third step $\Delta H^{\ddagger}_{-3}$ and $\Delta S^{\ddagger}_{-3}$ were determined to be 36 kcal/mol and 71 cal/mol K, respectively. The results are listed in Table 1.

Although the first second order process was too rapid for the values of the rate constants to be determined, the values of 4×10^8 M^{-1} s^{-1} and 8×10^3 s^{-1} were evaluated as the lower limit values of the forward and backward rate constants respectively. This calculation used the equilibrium constant $K'_1=5\times10^4$ M^{-1}

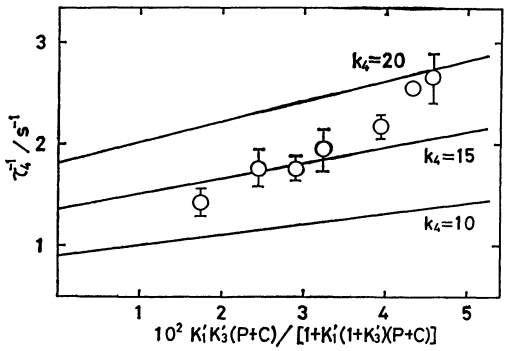

Fig. 7. Plot of τ_4^{-1} with Model 3.

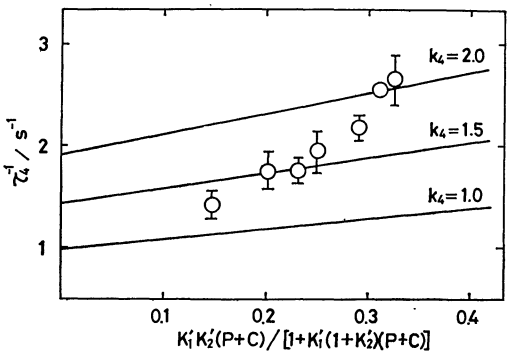

Fig. 8. Plot of τ_4^{-1} with Model 4.

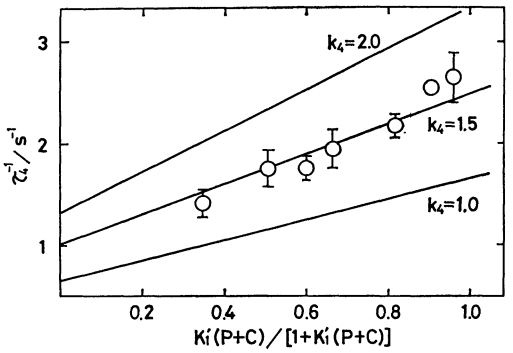

Fig. 9. Plot of τ_4^{-1} with Model 5.

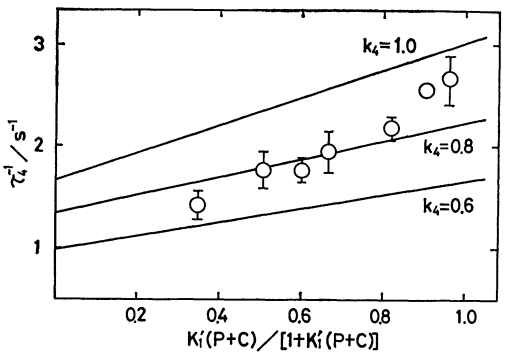

Fig. 10. Plot of τ_4^{-1} with Model 6.

Table 2. Binding constants of dyes to the highest affinity site of albumin

Bilirubin	Ref.	Bromphenol Blue	Ref.	Phenol Red	Ref.
7.0×10^{7} M^{-1} a)	21	1.5×10^{7} M^{-1} a)	23	1.1×10^{5} M^{-1} b)	24
2.7×10^{7} M^{-1} b)	5	1.4×10^{7} M^{-1} b)	present study	2.8×10^{4} M^{-1} a)	25
2.4×10^{7} M^{-1} a)	22	7.8×10^{5} M^{-1} b)	17	1.5×10^{4} M^{-1} a)	23
2.2×10^{7} M^{-1} b)	21				
1.5×10^{7} M^{-1} b)	22				

a) Human albumin. b) Bovin albumin.

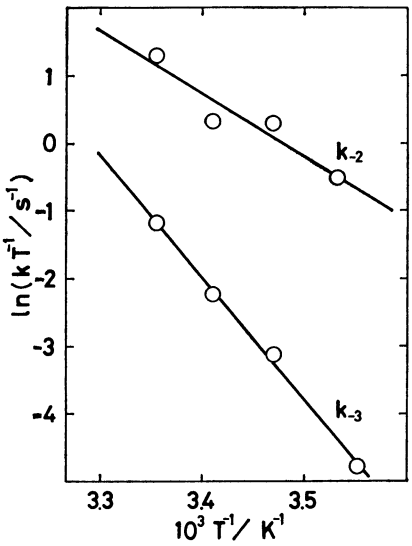

Fig. 11. Eyring plots of the rate constants.

estimated in the analysis of the slower processes, the time constant of the apparatus (100 μs), and the lowest observed concentration.

Discussion

The kinetic behaviour of the interaction of BPB with albumin is of interest in terms of competition binding with bilirubin. It was found from the present study that the binding of BPB to the primary binding site of BSA consists of many first order steps following a fast second order step. The multiplicity of the binding steps has also been observed in the case of the binding of bilirubin with albumin.[4,6] Reed *et al.*[19] have shown through peptic hydrolysis that bilirubin and Bromcresol Green bind to the same position on the BSA molecule, p-14 (residues 186—306). Bromphenol Blue and Phenol Red, which are sulfonphtalein dyes, have structures similar to that of Bromcresol Green, so that these dyes can be thought to bind to the same position. However, multiple binding steps for Phenol Red were not observed,[20] in contrast with the results of bilirubin and BPB. On the other hand, it can be seen from the comparison of the binding constants to the highest affinity site of albumin in Table 2 that the binding constants of bilirubin and BPB are about two or three orders of magnitude larger than that of Phenol Red. These facts seems to indicate the existence of a strong correlation between the multiplicity of the binding processes and the magnitude of the binding constant: that is, ligands having higher affinity bind in more steps than ligands having lower affinity. This can be interpreted as follows. The ligand molecule which has a large binding constant can migrate deeply into the hydrophobic crevice of the albumin molecule. For such a molecule, there must exist many barriers to be overcome during the migration. The existence of those barriers, which correspond to activated states, may yield multiple relaxations. This migration process seem to be driven by entropy rather than enthalpy, considering the insensitivity of the present system to temperature.

Although the reaction mechanism of the binding of BPB to BSA could not be uniquely determined from only the concentration dependences of the relaxation times, the series model (Model 1) seems to be more likely from the viewpoint of the stepwise migration of BPB into the deep site of the hydrophobic crevice of BSA molecule. The magnitude of the rate constant of the first association process was found to be larger than 4×10^{8} M^{-1} s^{-1} from the present analysis. This value suggests that the first association process is the diffusion controlled process. The rate constant of the dissociation process has also a relatively large value. Therefore, the first process can be thought of as the association-dissociation reaction of BPB at the cation rich hairpin turn located on the end of loop 2A[26] of the albumin molecule, which is governed by electrostatic forces. Moreover, the large value of K_4 suggests that there still exist complex formation processes in the longer time region. This can also be understood from the existence of the slow fifth process which was not analyzed in the present study.

From the analysis of the temperature dependences of the relaxation times, it was found that the activation entropies of the backward process in the second and third steps take positive values. This fact shows that those processes occur through the disordered activated states. On the other hand, Scheider[9] has reported for the association-dissociation reaction between oleate and human serum albumin that the first order process which follows the assumed fast second order process occurs with a negative activation entropy, that is, through the ordered activated state. He has pointed out two possibilities for the role of the ligand in the activated configuration. One possibility is that the ligand plays no role in activation *i.e.*, the protein can take the activated configuration on a purely probabilistic basis without any ligand help. The other is that the ligand is closely involved in the activation process *i.e.*, the ligand's movement on the exterior surface brings it to the mouth of the hydrophobic

crevice, facilitating the formation of the activated configuration. Considering both results, it can be seen that the different ligand species yield different activated configurations, and we may consider that the ligand is closely involved in the activation process. If the present argument is correct, the difference in albumin between the two studies may not be the decisive factor to explain the characteristically different results.

In the present analysis, it was assumed that the extinction coefficients of BPB in all the complexes have the same value. This assumption should be regarded as a first approximation. Strictly speaking, each extinction coefficient probably has a different value. To take account of this difference in the consideration of the reaction mechanism, ε_i, ΔV_i, K_i', which are, respectively, the extinction coefficient of the ith complex, the volume change and the equilibrium constant of the ith process, must be determined by simulation using the data of the concentration dependence of the relaxation amplitudes along with the relaxation times. However, the relaxation amplitudes of the present system are too small for us to get data of enough accuracy to perform the above mentioned simulation.

References

1) A. Froese, A. H. Sehon, and M. Eigen, *Can. J. Chem.*, **40**, 1786 (1962).
2) J. M. Thorp, "Absorption and Distribution of Drugs," ed by T. B. Binns, E. & S. Livingstone L. T. D. Edinburgh and London (1964), Chap. 4.
3) M. C. Meyer and D. E. Guttman, *J. Pharm. Sci.*, **57**, 895 (1968).
4) R. F. Chen, *Arch. Biochem. Biophys.*, **160**, 106 (1974).
5) T. Faerch and J. Jacobsen, *Arch. Biochem. Biophys.*, **168**, 351 (1975).
6) T. Faerch and J. Jacobsen, *Arch. Biochem. Biophys.*, **184**, 282 (1977).
7) R. G. Reed, *J. Biol. Chem.*, **252**, 7483 (1977).
8) R. D. Gray and S. D. Stroupe, *J. Biol. Chem.*, **253**, 4370 (1978).
9) W. Scheider, *Proc. Natl. Acad. Sci. U. S. A.*, **76**, 2283 (1979).
10) R. Flores, *Anal. Biochem.*, **88**, 605 (1978).
11) H. Hertz, *Scand. J. Clin. Lab. Invest.*, **35**, 545 (1975).
12) H. Hertz, *Scand. J. Clin. Lab. Invest.*, **35**, 561 (1975).
13) V. P. Dole, *J. Clin. Invest.*, **35**, 150 (1956).
14) K. Hachiya, M. Ashida, M. Sasaki, H. Kan, T. Inoue, and T. Yasunaga, *J. Phys. Chem.*, **83**, 1866 (1979).
15) G. Scatchard, *Ann. N. Y. Acad. Sci.*, **51**, 660 (1949).
16) O. J. Bjerrum, *Scand. J. Clin. Lab. Invest.*, **22**, 41 (1968).
17) H. Peeters, M. Y. Rosseneu-Motreff, and F. Soeteway, *Protides Biol. Fluids, Proc. Colloq.*, **20**, 471 (1973).
18) L.-O. Anderson, A. Rehnström, and D. L. Eaker, *Eur. J. Biochem.*, **20**, 371 (1971).
19) R. G. Reed, R. C. Feldhoff, O. L. Clute, and T. Peters, Jr., *Biochemistry*, **14**, 4578 (1975).
20) D. E. Goldsack and P. M. Waern, *Can. J. Biochem.*, **51**, 1281 (1973).
21) R. F. Chen, "The Fluorescence of Bilirubin-Albumin Complexes," in "Fluorescence Techniques in Cell Biology," ed by A. A. Thaer and M. Sernetz, Springer-Verlag, New York (1972), p. 273.
22) J. Krasner, G. P. Giacoia, and S. J. Yaffe, *Ann. N. Y. Acad. Sci.*, **226**, 101 (1973).
23) U. Kragh-Hansen, J. V. Møller, and K. E. Lind, *Biochim. Biophys. Acta*, **365**, 360 (1974).
24) F. L. Rodkey, *Arch. Biochem. Biophys.*, **94**, 38 (1961).
25) F. L. Rodkey, *Arch. Biochem. Biophys.*, **94**, 526 (1961).
26) J. R. Brown, "Serum Albumin; Amino Acid Sequence," in "Albumin Structure, Function and Uses," ed by V. M. Rosenoer, M. Oratz, and M. A. Rothchild, Pergamon, New York (1977), p. 27.